Lehrstuhl für
Kontinuumsrobotik

Leibniz
Universität
Hannover

Summer Research Internship

Shape Sensing of Tubular Continuum Robots using Stereo Vision

Priyanka Rao
Indian Institute of Techonology, Madras

Hanover, July 26, 2017

Supervisors :
Prof. Dr.-Ing. Jessica Burgner-Kahrs
Dr. M. Taha Chikhaoui

Contents

1 Introduction **2**

2 Calibration and Base detection **2**

3 Backbone extraction **3**

3.1 Backbone segmentation 3

3.1.1 Rough estimate of location of backbone 3

3.1.2 Segmentation of the tube 4

3.2 Backbone points extraction 6

3.2.1 Thinning 6

3.2.2 Labelling of points 6

4 3D reconstruction **7**

5 Parameter identification **7**

5.1 Diameter measurement 8

5.1.1 3d interpolation 9

5.1.2 Epiline approximation 10

5.2 Segment identification 10

5.3 Shadow removal 12

5.4 Rotation angle 14

6 Conclusion **14**

Abstract

Accurate steering of tubular continuum robots for complex surgical procedures requires precise and robust determination of its shape and pose. However, due to characteristics such as friction, nonlinear elasticity, hysteresis, actuation and other environmental uncertainties, the expected shape and pose estimated by the forward-kinematic model of concentric tube continuum robots fail to be accurate. This project aims to overcome this by performing shape sensing of a continuum robot using stereo-vision modality.

1 Introduction

There are multiple state of the art devices that can be used to perform shape sensing on a continuum robot. For example, FARO arm is a portable coordinate measuring machine that can uses tactile sensing to obtain a point cloud of the robot. However, it cannot be used as an online measurement system. Similarly, Fiber Bragg grating (FBG) sensors use strain at every FBG cross section to reconstruct the backbone from the curve parameters at each cross section. They can be used for both continuous and online measurements but are expensive and are still being explored for estimating complex shapes. Aurora sensors use electromagnetic tracking to compute the pose of the coil. While they can be used for online measurements, they cannot be used to obtain continuous measurments and are prone to errors due to magnetic field distortions. The following project aims to eliminate the above problems by performing online, continuous measurements using stereo vision. It is a continuation of Marc Schlenker's master thesis on the same topic. The project is aimed at building a standalone C++ program for online measurement of parameters of tubular continuum robots.

2 Calibration and Base detection

Calibration data for 2D and 3D setup was obtained from the previously implemented GUI. The fundamental matrix,distortion coefficients and 2D calibration data for each camera is stored in "2d-calibration.xml" while the 3D camera calibration data is saved in the "3d-calibration.yml" file.

The four ArUco markers are used to set the Base co-ordinate system for the setup. Center of Marker Id 2 is considered as the origin and the X and Y axes are as shown in Figure 1, with the Z axis perpendicular to the base.

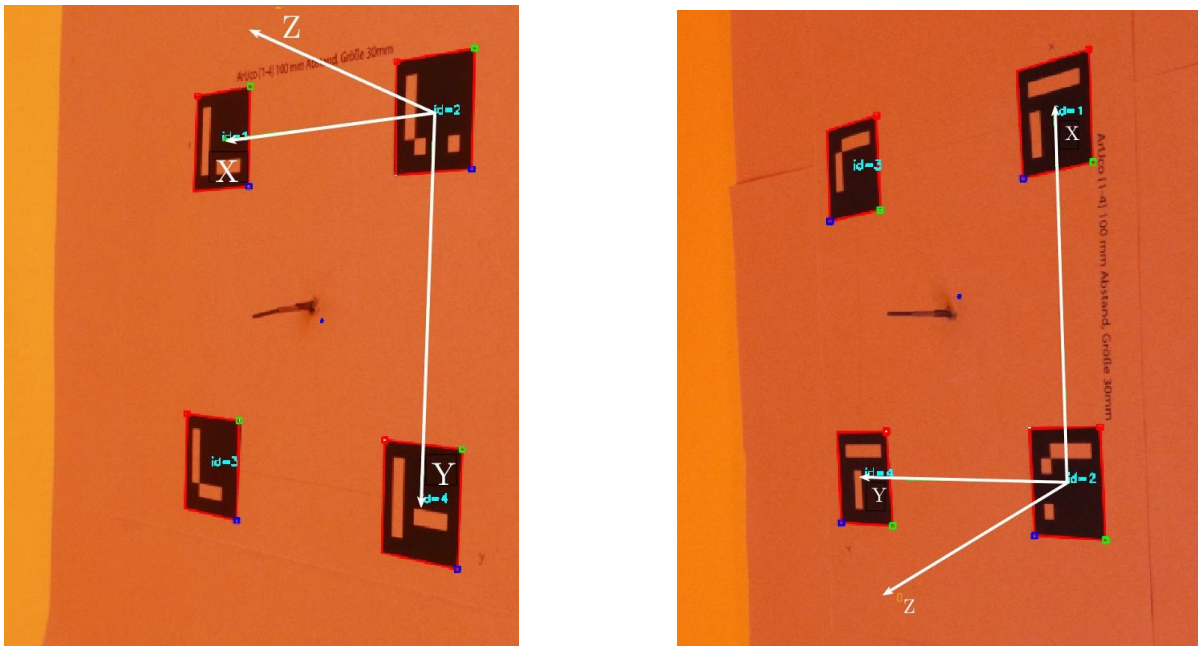

Figure 1: Detected ArUco markers in images from both the cameras with their X, Y and Z axes marked

3 Backbone extraction

The next step involves segmentation of the robot alone from the images obtained. Once achieved, the points along its backbone can be determined using thinning to obtain the 3D coordinates of the backbone.

3.1 Backbone segmentation

3.1.1 Rough estimate of location of backbone

The existing method thresholds the image by using a Background Chroma Key by moving over the entire image, pixel by pixel. For faster computation when the system is used online, floodfill function has been used which reduces the execution time by a factor of 100. Floodfill is used to color area consisting of connected pixels with the same color range. Since this method does not have a tight threshold, variation in the location of base center should not affect the segmentation significantly. It has not been integrated into the existing framework yet.

The blue rectangle in Figure 2 gives the Region of Interest (ROI) containing the location of the backbone.

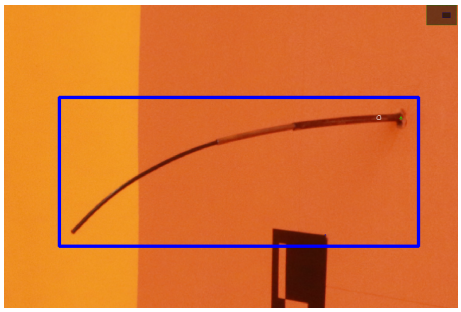

Figure 2: Estimation of the ROI containing location of the backbone,enclosed within the blue rectangle

3.1.2 Segmentation of the tube

By using a background Chroma Key, obtained as input from the User, the image is thresholded to remove the background. The tolerance selected must ensure that the thresholded image of the backbone does not include noise and shadows. The entire tube must be extracted.

Canny edge detection is applied to obtain the edges. Due to reflective nature of the metal tube, a lower tolerance for the Chroma key is required to be given as input for background subtraction. This causes the shadow cast by the tube to be segmented out along with the tube as shown in Figure 3.

Figure 3: Tube extraction after background subtraction using a Chroma Key

Applying Hough transform at an ROI near the Base Center, we can estimate the base of the tube as its sides can be approximated as straight lines. Creating a base mask using the area in the intersection between the detected lines and the ROI, we can obtain the extracted backbone without the noise at the base . Figure 4 shows the ROI around the base center.

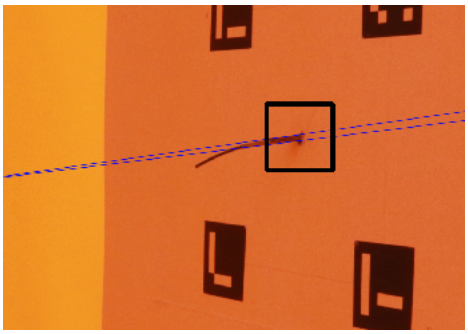

Figure 4: The ROI around the base center is indicated by the black rectanlge. The blue lines indicate the straight lines detected by Hough transfrom

The centroid of the base mask (see Figure 5) can be used as the seed point for applying floodfill to the thresholded image, thus eliminating the need for the robot to be precisely located at the center of the ArUco markers.

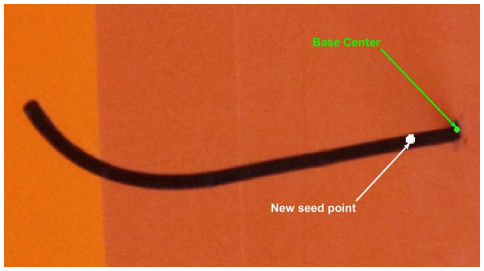

Figure 5: Base Center is indicated in green and the new seed point obtained is indicated in white

However, this method is efficient only if the extracted image after Background subtraction is done successfully and is free of shadows and noise. Figure 6 shows a tube that has not been extracted well. Hough transform to detect the tube base fails in such cases.

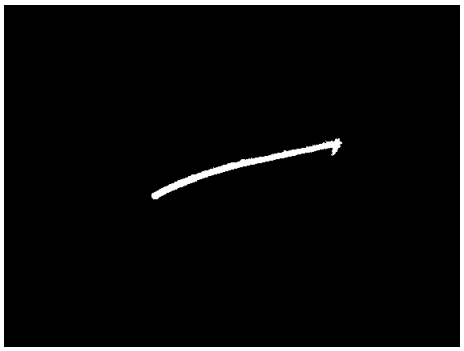

Figure 6: Segmented tube with noise at the base

3.2 Backbone points extraction

After obtaining the segmented robot from the image, thinning needs to be performed to extract the backbone. Once all the pixels are obtained, it is necessary to relabel the backbone points, starting from the base.

3.2.1 Thinning

A fast parallel algorithm for thinning by Zhang et al. [1] has been used. It is used to obtain a skeleton of the extracted backbone and is of unitary pixel thickess. Each pixel indicates a point on the backbone and can be used for further processing.

3.2.2 Labelling of points

It is important that the backbone points are arranged in a sequential order as they are used to calculate the radius of curvature of the backbone. The exisiting algortihm uses the distance from the Base center[1] as a criterion to sort the detected backbone points. However, this method fails if the end effector is curved backwards, as shown in Figure 7.

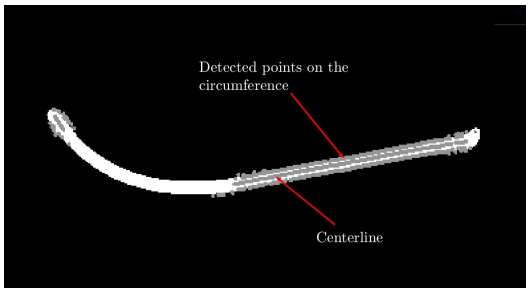

Figure 7: Snapshot of failed continuous ordering of backbone points at an intermediate stage

The current version ignores all the pixel points to the right of the Base center and starts searching and indexing points to its left. It considers the point closest to the Base center as first point and searches its 8 neighbouring pixels for the next point. Figure 8 indicates the correct labelling of points without the discontinuities observed in Figure 7.

[1]Base center refers to the center of the centers of the ArUco Markers (see Figure 1)

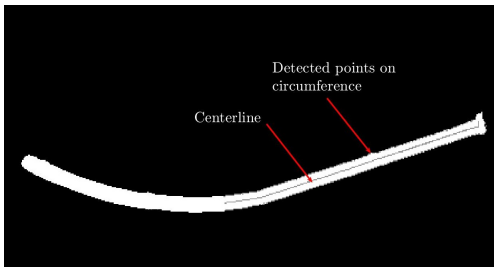

Figure 8: Snapshot of successful intermediate ordering of backbone points, without discontinuities

4 3D reconstruction

Implementation of existing code has been done, resulting in a 3D point cloud of the backbone points as shown in Figure 9.

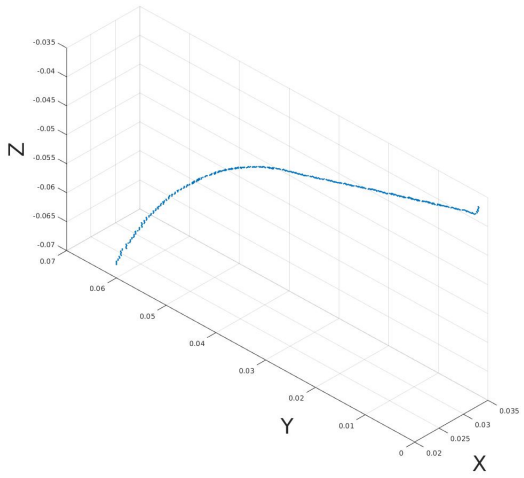

Figure 9: Backbone points obtained

5 Parameter identification

Configuration space variables of a continuum robot are curvature, angle of the plane containing the curvature and the length of the arc. Radii of each segment of a tubular continuum robot also need to be measured in order to identify the position of each segment. All of the above parameters, excluding length and curvature of the arc have been identified and measured.

5.1 Diameter measurement

Majority of methods involving direct interpolation failed when the robot's end effector was oriented out of the plane of the camera, towards/away from it. For example, consider a single tube with its end curved towards the camera as shown in Figure 10.

Figure 10: Example of a tube where the tip is angled towards the camera. The observed radius at the tip is more than the observed radius of the rest of the tube

Even though the tube is of constant radius, the number of pixels measured as radius increases as we move away from the base. If radius is considered directly proportional to the number of pixels measured, the above case will measure a constant increase in radius as shown in Figure 11.[2]

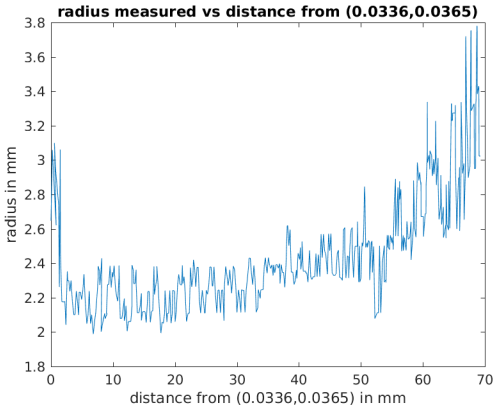

Figure 11: Radius measured for the example in Figure 10

[2]The offset of fifth backbone point has been chosen to avoid selecting a point in the bakcbone that has been segmented due to shadows or other noise.

5.1.1 3d interpolation

Consider n backbone points with $(x_i, y_i, z_i)^T$ as their world 3D coordinates. Assuming that the two views are exactly perpendicular, this method assumes that the radius of the tube at the i^{th} point can be directly interpolated from the distance between the $i^{th}$and the $i+1^{th}$point. Let $i^{th}$and the $i+1^{th}$points be under consideration. Let p_1 and p_2 be the pixel distances between them in both the stereo images. Let d_{p1} and d_{p2} be the diameters of the tube measured in pixels in the stereo images. Image i_1 and Image i_2 indicate images from stereo cameras 1 and 2 respectively. All the As seen in Figure 1, this method assumes that only the Y and Z co-ordinates in Image i_1 and the X and Z co-ordinates in Image i_2 are significant.

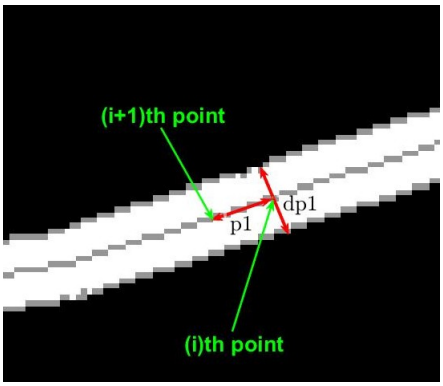

Figure 12: Various notations indicated in i_1

Considering Image1 indicates only the Y annd Z world co-ordinates and Image 2 the X and Z co-ordinates (difference in X and Y co-ordinates in respective views assumed negligible), diameter in the real world co-ordinates, d_s can be approximated by

$$d_{s2} = \frac{((x_i - x_{i+1})^2 + (z_i - z_{i+1})^2) * d_{p2}}{p_2}$$

$$d_{s1} = \frac{((y_i - y_{i+1})^2 + (z_i - z_{i+1})^2) * d_{p1}}{p_1}$$

$$d_s = \frac{d_{s2} + d_{s1}}{2}$$

Figure 13 indicates the various diameters obtained for a single tube with a diameter of 2.4 mm.

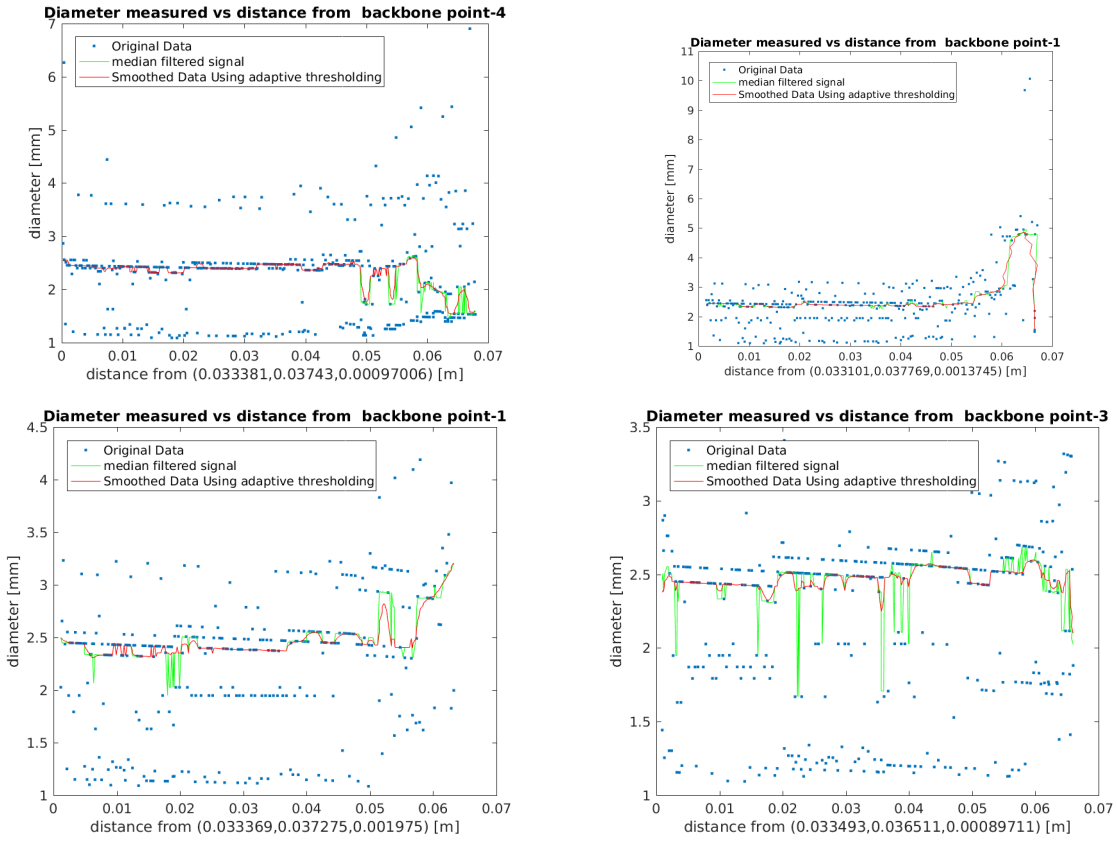

Figure 13: Segmentation at various configurations of a tube with single radius

5.1.2 Epiline approximation

Consider a point on the surface of a backbone in Image i_1 . Since the tube is symmetric, it is not possible to pinpoint its exact location in Image2. However, we know that it lies in the region of intersection between the tube and its corresponding epiline in Image i_2 . By computing the 3D co-ordinates of the point in Image i_1 and the points in the ROI in Image i_2 , the point with minimum distance from the corresponding backbone point can be used to calculate the diameter.

However, this method yielded measurements lower than the ground truth and hence was discarded. However it can be tried if a larger tolerance for thresholding the images is used.

5.2 Segment identification

With the previous algortihm, only pixels were measured in both the images to distinguish between segments as shown in Figure 14.

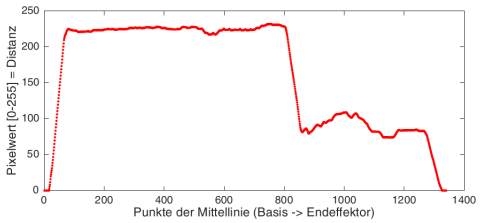

Figure 14: Previously implemented radius measurement

With the method implemented in Section 4.1.1, the following radii (see Figure 15) were measured as well as the segments clearly distinguished in both the 3D reconstruction and the thresholded 2D images. The measurements have been filtered in order to reduce noise. Figure 16 indicates the different detected segments in the tubular continuum robot.

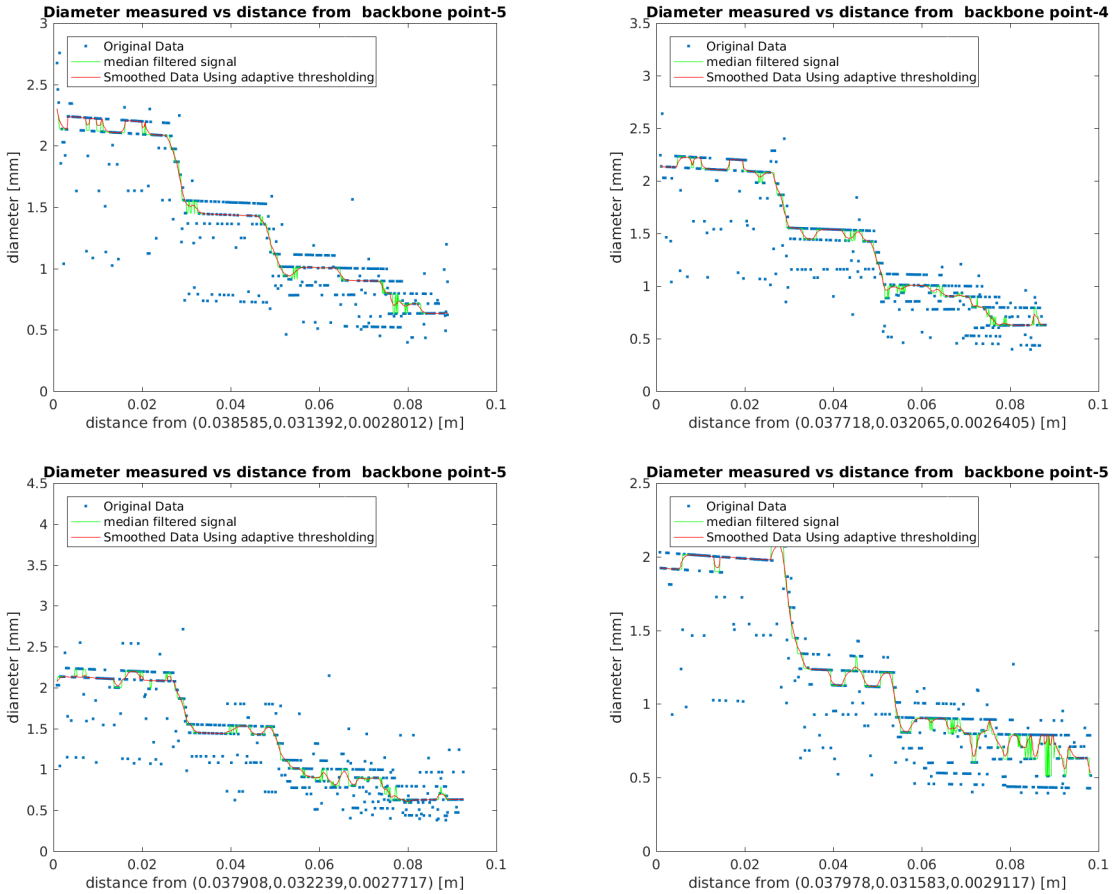

Figure 15: Segmentation at various configurations of a continuum robot with 3 tubes

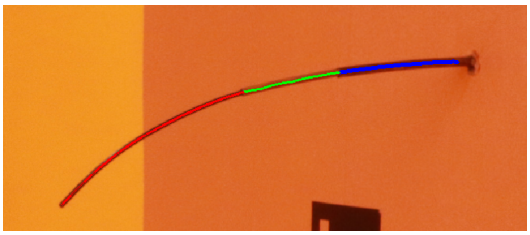

Figure 16: Highlighted detected segments of the robot

However the measurement fails if the robot is not extended outward enough as shown in the Figure 17 .

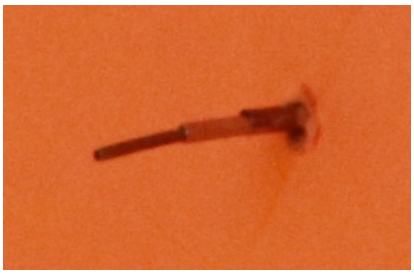

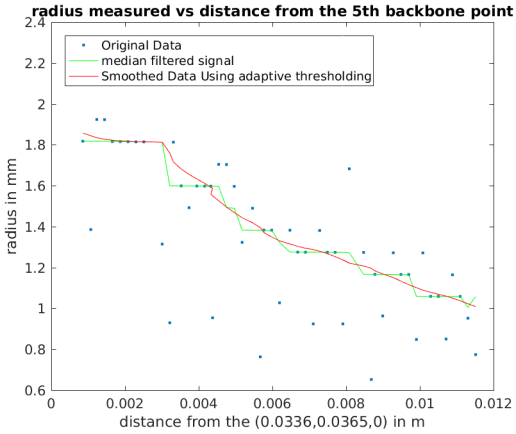

Figure 17: The orientation and correspoding diameter measurement are shown in the left and right images respectively

5.3 Shadow removal

Consider n backbone points, where data containts the real world 3D co-ordindates of the backbone points. Let j be the increment considered for calculation of slope. It is advisable to consider j>1 to prevent noise interference. First iteration begins by considering the slope between the first and the $(1+j)^{th}$ point as the reference slope.

Algorithm 1 Segmentation

```
refSlope← data(1+j)-data(1)
for a→ 2 to n-j-1
   currData← data(a)
   currSlope← data(a+j)-currData
   currAngle← acosd(dot(currSlope,refSlope))
   if (currAngle) > tolerance
      dumpSlope← data(a+1+j)-currData
      dumpAngle← acosd(dot(dumpSlope,refSlope))
       if(abs(dumpAngle)>tolerance)
         startSegment← currData
         segCol ← 1
         segRow← segRow+1
         segmentMatrix(segRow,segCol)← a
         refSlope← data(a+j)-startSegment
       else
         segCol← segCol+1
         segmentMatrix(segRow,segCol)← a
       end if
   else
      segCol← segCol+1
      segmentMatrix(segRow,segCol)← a
   end if
end for
```

The above algorithm is effective in identifying the convexity defect caused due to the segmentation of shadow along with the tube. In Figure 18 the start of each segment identified by Algorithm 1 is indicated. The segment belonging to the shadow can be ignored to correctly identify the start of our backbone. Tolerance angle indicates the deviation of a point from the reference slope and determines the sensitivity of the segments detected. Higher tolerance will result in segregation into lesser number of segments. Figure 18 indicates the segments identified with different tolerances.

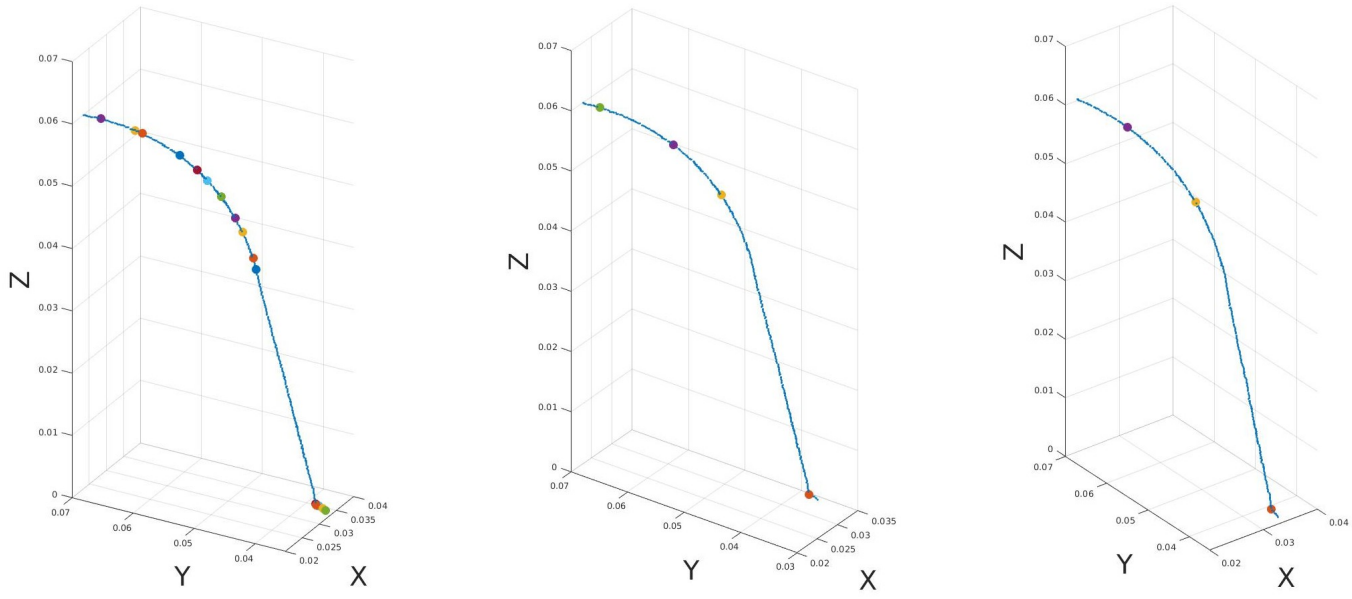

Figure 18: Segmentation with tolerances 10^o,20^o and 30^o respectively

5.4 Rotation angle

One of the parameters required to describe a tubular continuum robot is ϕ, where ϕ indicates the angle made by the plane containing the curvature with the X-Z plane. From the obtained 3D points of the backbone, a plane is fitted for points lying in the same segment, assuming that there is not distortion of the backbone. Due to mounting errors, the experimental data does not have the robot perpendicular to the base. Hence the following three parameters have been identified,

ϕ_{XY}, angle made by the plane with the X-Y plane

ϕ_{ZX}, angle made by the plane with the Z-X plane

ϕ_{YZ}, angle made by the plane with the Y-Z plane

6 Conclusion

Reimplementation and modification of Marc Schlenker's master thesis has been completed. Diameter measurement has been achieved with a maximum error of 6.76% for a diameter of 2.4 mm. A method of rough estimation using OpenCV's floodfill function has been implemented which reduces the processing time by a factor of $\frac{1}{100}$. It has not been integrated yet. An effective method for shadow removal, segment differentiation and rotation angle calculation has been incorporated.

Further work will include conversion of parameter analysis into real time C++ code, further study of Section 5.1.2, incorporation of Section 3.1.1 for faster processing speed and effective segmentation of the backbone into straight lines and arcs for further parameter detection.

References

[1] T. Y. Zhang, C. Y. Suen,'A Fast Parallel Algorithm for Thinning Digital Patterns, 1984

[2] Prof. Dr.-Ing. Jessica Burgner-Kahrs' lecture on Continuum Robotics, Leibniz University of Hanover, 2016